LETTER

Methane emission offsets carbon dioxide uptake in a small productive lake

Dominic Vachon [iD],[1,2]* Timon Langenegger [iD],[1] Daphne Donis,[1] Stan E. Beaubien [iD],[3] Daniel F. McGinnis [iD][1]

[1]Aquatic Physics, Department F.-A. Forel for Environmental and Aquatic Sciences (DEFSE), Faculty of Sciences, University of Geneva, Geneva, Switzerland; [2]Department of Ecology and Environmental Science, Umeå University, Umeå, Sweden; [3]Dipartimento di Scienze della Terra, Università di Roma "La Sapienza", Roma, Italy

Scientific Significance Statement

Carbon budgets of natural and impacted ecosystems, including lakes, are critical to quantify their role in regulating Earth's climate. Excessive nutrient loading to lakes both increases their algal production resulting in atmospheric CO_2 uptake and increases CH_4 production due to anaerobic decomposition of organic matter. The net balance between CO_2 uptake and CH_4 emissions from lakes, however, has not been extensively addressed. Our work reveals that a substantial proportion of the organic carbon supplied by the net ecosystem production is used for methanogenesis and emitted back to the atmosphere as CH_4. From a climate change perspective, exchanging CO_2 uptake with CH_4 release is an "unfair trade" for the atmosphere, as CH_4 has a much greater global warming potential than CO_2.

Abstract

Here, we investigate the importance of net CH_4 production and emissions in the carbon (C) budget of a small productive lake by monitoring CH_4, CO_2, and O_2 for two consecutive years. During the study period, the lake was mostly a net emitter of both CH_4 and CO_2, while showing positive net ecosystem production. The analyses suggest that during the whole study period, 32% ± 26% of C produced by net ecosystem production was ultimately converted to CH_4 and emitted to the atmosphere. When converted to global warming potential, CH_4 emission (in CO_2 equivalents) was about 3–10 times higher than CO_2 removal from in-lake net ecosystem production over 100-yr and 20-yr time frames, respectively. Although more work in similar systems is needed to generalize these findings, our results provide evidence of the important greenhouse gas imbalance in human-impacted aquatic systems.

Constraining uncertainties of the various carbon (C) sources and sinks of natural and human-impacted systems is critical to understand their impact on the Earth's climate (Le Quéré et al. 2018; Nisbet et al. 2019). By emitting and storing C, freshwater systems have a significant role in the global C cycle (Battin et al. 2009), which can be altered by anthropogenic forcing (Tranvik et al. 2009; Regnier et al. 2013). For example, productive systems affected by nutrient loading can remove CO_2 from the atmosphere and store this organic C in their sediments (Anderson et al. 2014; Pacheco et al. 2014). At the same time, productive lakes and reservoirs have been shown to release CH_4 globally (DelSontro et al. 2018). As CO_2 and CH_4 are two important greenhouse gases (GHGs) with different atmospheric warming potentials, a deeper understanding of their coupled cycle in productive freshwater ecosystems is paramount to better evaluate their potential role for the Earth's climate system.

Freshwater CH_4 emissions are usually less substantial than CO_2 fluxes (Bastviken et al. 2011); however, CH_4 has a warming potential 28 and 84 times greater than CO_2 over 100-yr and 20-yr time frames, respectively (Myhre et al. 2013). Although CH_4 production can be relatively important in surface waters (Günthel et al. 2019), most production occurs in anoxic environments, such as isolated bottom waters and sediments, and is mostly fueled by excess organic matter from primary production (Kelly and Chynoweth 1981; West et al. 2012). Other factors like temperature (Yvon-Durocher et al. 2014), hydrodynamics (Vachon et al. 2019*a*), and the availability of other oxidants (e.g., nitrate, sulfate, and ferric iron) also affect CH_4 dynamics in freshwater systems. The link between productivity and CH_4 emissions has been shown empirically in various freshwater systems (Whiting and Chanton 1993; DelSontro et al. 2016); however, the net balance between CO_2 uptake by positive net ecosystem production and CH_4 emissions has not been extensively addressed and may have critical implications on the net GHG atmospheric exchange balance.

Here, we evaluate the contribution of CH_4 production to the whole-lake C cycle in a small productive lake (Soppensee, Switzerland). Due to the high primary productivity and extended bottom anoxia found in this lake (Vachon et al. 2019*a*), we hypothesized that fresh organic matter production in the summer leads to substantial CH_4 production, which may significantly offset net CO_2 uptake by ecosystem production. We test this by applying a mass balance approach using high-frequency measurements, including vertical profiles of O_2, CO_2, and CH_4 concentrations and surface fluxes for two consecutive years, to derive whole ecosystem net gas production rates and to determine the fraction of organic carbon input that is ultimately converted to CH_4.

Materials and methods

Study site and background limnological information

The study was conducted in the small eutrophic lake Soppensee (47.09°N, 8.08°E) situated in the Canton Lucerne, Switzerland (lake area: 23 ha, maximum depth: 26 m, mean depth: 12.2 m) during the years 2016 and 2017 (meteorological conditions shown in Supporting Information Fig. S1 were provided by the Swiss Federal Office of Meteorology and Climatology). The lake basin is characterized by steep sides and a relatively flat bottom and the drainage basin (1.6 km^2) is mainly occupied by agricultural land (Lotter 1989). The water residence time is about 3.1 yr (Gruber et al. 2000). In 2016–2017, total phosphorus measured spectrophotometrically after potassium persulfate ($K_2S_2O_8$) digestion, was on average ($\pm$ 1 standard deviation [SD]) $28 \pm 16\ \mu$g P L^{-1} in the surface water and $71 \pm 15\ \mu$g P L^{-1} when integrated over the whole water column. Dissolved organic carbon was more equally distributed in the water column, with an average ($\pm$ 1SD) of 5.2 ± 0.5 mg C L^{-1} (Canton of Lucerne pers. comm.). The lake was strongly thermally stratified from May to October each year, after which the water column mixed partially in winter 2016/2017 (with ice cover) and completely in winter 2017/2018. Vertical profiles of water temperature and conductivity, as well as a more detailed physical description of the water column, are provided in Vachon et al. (2019*a*).

Dissolved O_2, CO_2, and CH_4 measurements

Dissolved O_2 and CO_2 sensors were deployed at about 1.5 m depth on a mooring situated at the deepest point of the lake. The dissolved O_2 probe (optode, miniDOT, Precision Measurements Engineering, range = 0–150% saturation, accuracy = $\pm$ 10 μmol L^{-1}) logged temperature, dissolved O_2 concentration (mg O_2 L^{-1}), and saturation (%) every minute. CO_2 partial pressure (pCO$_2$, μatm) was measured every hour by a GasPro probe (detection limit between 10 and 20 μatm) (Graziani et al. 2014). Both probes were fitted with a copper mesh to prevent biomass growth. The measurement of pCO$_2$ is based on equilibration of the surrounding water with a small-volume headspace containing a miniature nondispersive infrared (NDIR) detector (model IRC-A1; Alphasense) via diffusion through a gas permeable membrane (Teflon AF 2400; Biogeneral). Continuous pCO$_2$ measurements were not available from April 2016 to July 2016 and from September to November 2016. During those periods, daily pCO$_2$ values were linearly interpolated.

In addition to high-frequency measurements from the loggers, profiles of dissolved gases were performed approximately on a monthly basis at the deepest point of the lake. Dissolved O_2 profiles were measured using a multiparameter sonde (Yellow Spring Instrument EXO2, after May 2017 a Seabird CTD profiler, SBE19) and a 1 m resolution was used for the mass balance calculation. Dissolved CH_4 and CO_2 in the water column were measured using the headspace method (Tang et al. 2018; Vachon et al. 2019*a*). Dissolved inorganic carbon (DIC) concentrations were derived from CO_2 and alkalinity (Alk) using water temperature and the carbonate system dissociation constants (Stumm and Morgan 1995). More details are provided in Supporting Information Section S1. All dissolved

gases measurements data are available in the Dryad data repository (Vachon et al. 2020).

Gas fluxes with the atmosphere

Surface diffusive fluxes of CH_4 (F_{CH4}) and CO_2 (F_{CO2}) at the air–water interface were measured using a floating chamber connected in a closed-loop to a portable greenhouse gas analyzer (Los Gatos Research, California, U.S.A.) as described in McGinnis et al. (2015). During each sampling campaign, a series of 3–9 chamber deployments were performed during the day (between 09:00 h and 16:00 h) from an anchored boat at the center of the lake ($n = 136$). From these diffusive flux measurements, 74 and 84 measurements were performed in combination with surface-water measurements of dissolved CO_2 and CH_4 concentrations, respectively. These combined flux and dissolved concentration measurements were used to calculate the gas transfer velocity (k) to develop specific wind-k models (*see* Section S2 and Fig. S2 in Supporting Information). These models (one derived from CO_2 and the other from CH_4) were used to estimate daily surface diffusive fluxes (F_X, where X is either O_2, CO_2, or CH_4; mmol m^{-2} d^{-1}) using Fick's First Law of diffusion as $F_X = k_X([X]_{sw} - [X]_{eq})$. k_X is the gas transfer velocity (m d^{-1}) derived from the specific wind-based model (k derived from CH_4 was used for O_2 and CH_4 fluxes, and k derived from CO_2 was used for CO_2 fluxes), $[X]_{sw}$ is the surface-water O_2, CO_2, or CH_4 concentration and $[X]_{eq}$ is the O_2, CO_2, or CH_4 concentration in equilibrium with the atmosphere calculated using Henry's Law with water temperature. Model-derived k_{600} (standardized for CO_2 at 20°C) were converted to gas specific k_X using gas Schmidt numbers estimated from surface-water temperature and using an n exponent of $-2/3$ for smooth surfaces and $-1/2$ for rough surfaces (Jähne et al. 1987).

We measured ebullition fluxes using five bubble traps made of inverted funnels with collectors deployed at various depths (Vachon et al. 2019a). Total gas flux (mmol m^{-2} d^{-1}) received by each funnel was calculated by accounting for funnel area, gas volume sampled, and deployment duration (usually 20–30 d). Total gas flux was multiplied by the fraction of CH_4 found in the bubbles collected locally from the sediment. The proportion of CH_4 fraction in the sediment bubbles was measured at various depths (Langenegger et al. 2019) and the proportion left at the surface was estimated using a discrete bubble model (McGinnis et al. 2006). Methane ebullition fluxes were extrapolated to the whole lake area by allocating the five funnel-derived results to five different bathymetric zones (more detailed information is provided in Supporting Information Section S3).

Net gas production calculation

We used O_2, CO_2, DIC, and CH_4 profiles and continuous surface fluxes to estimate the rates of net gas (or DIC) production using the following mass balance approach: $netX_{prod} = \frac{\Delta X_{mass}}{\Delta t} + surface \times flux$, where X is O_2, CO_2 (and DIC),

or CH_4. The argument $\frac{\Delta X_{mass}}{\Delta t}$ corresponds to the change in the whole water column X mass (mmol m^{-2}) between the two sampling days. Whole water column masses of dissolved O_2, CO_2, DIC, and CH_4 (mmol m^{-2}) for each sampling date were calculated by summing the gas masses (mmol) of each 1 m strata (concentration multiplied by the volume of the strata) and then dividing by the lake surface area (m^2). For this, CO_2, DIC, and CH_4 concentrations had to be linearly interpolated between sampled depths (whereas O_2 was measured at each meter). The daily surface fluxes for each gas were summed for each period (mmol m^{-2}). In winter 2016–2017, all gas fluxes with the atmosphere were set to 0 during the ice-covered period. For the DIC mass balance, integrated surface CO_2 flux from daily estimates was used. For $netCH_{4prod}$, the surface CH_4 flux is the integration of daily diffusive flux and ebullition rates. Integrated rates of net gas production were estimated for each period ($\Delta t \sim 20$–30 d) between two sampling dates (total of 20 periods). Daily rates of net gas production (mmol m^{-2} d^{-1}) were calculated by dividing by the number of days in each period. All fluxes and net gas production rates uncertainties were evaluated from k_{600} and gas measurement uncertainties using a Monte Carlo resampling procedure (Supporting Information Section S4).

Results

Gas dynamics and atmospheric exchange

Dissolved gases measured in the center of Soppensee were highly dynamic among seasons and showed strong vertical variation due to thermal stratification (Fig. 1). The water column was mostly anoxic under 10 m depth ($O_2 < 10$ μmol L^{-1}) from May to October of both years, while surface-water O_2 concentrations varied from oversaturation in summer to undersaturation in fall and winter (Supporting Information Fig. S3). Dissolved CO_2 and CH_4 accumulated in the bottom waters to reach concentrations of about 1.2 mmol L^{-1} and 1.3 mmol L^{-1}, respectively (Fig. 1). In the surface waters, CO_2 was oversaturated with respect to atmospheric concentration, except in September and October 2016 and summer 2017 (Supporting Information Fig. S3a). Surface-water CH_4 was consistently oversaturated during the summer months with measured concentrations ranging from 0.5 μmol L^{-1} to 1.5 μmol L^{-1} and from 0.8 μmol L^{-1} to 1.2 μmol L^{-1} in 2016 and 2017, respectively (Supporting Information Fig. S3b). During fall turnover, surface-water dissolved CO_2 and CH_4 concentrations drastically increased up to about 250 μmol L^{-1} and 50 μmol L^{-1}, respectively.

Daily modeled air–water diffusive CO_2 and O_2 fluxes both showed fluctuation between efflux (positive values) and influx (negative values), while CH_4 was being consistently emitted (except during the ice-covered period; Fig. 2). Average of modeled CO_2 and O_2 fluxes during the stratified season (May–October) was higher in 2016 (average $\pm$ 1 SD; 35.7 $\pm$ 31.9 mmol CO_2 m^{-2} d^{-1} and 64.0 $\pm$ 72.9 mmol O_2 m^{-2} d^{-1}) compared to 2017 (average $\pm$ 1 SD;
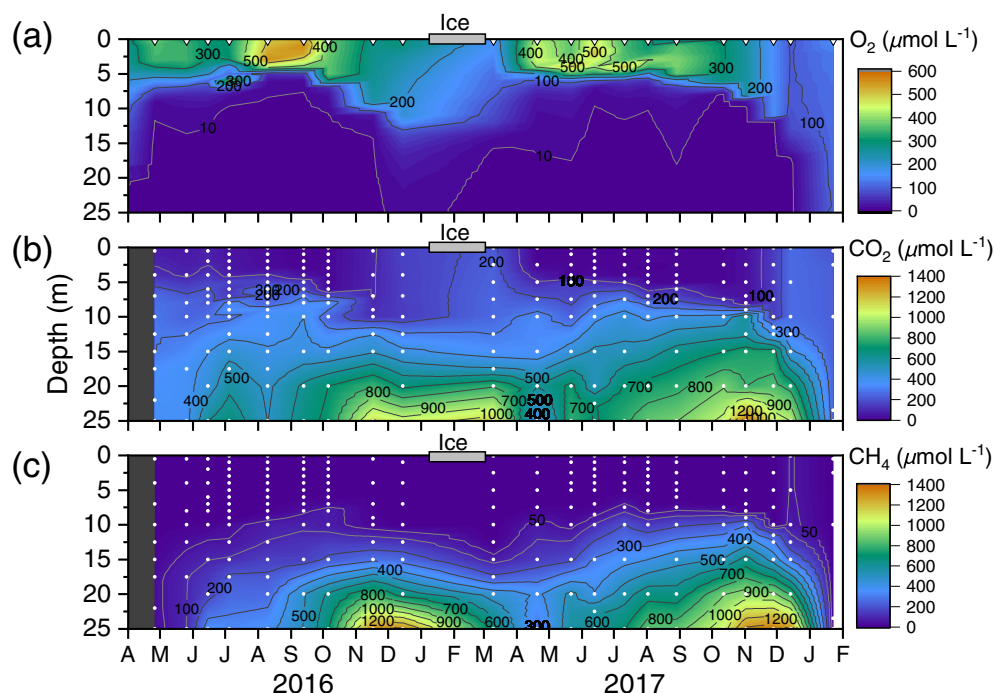
Fig 1. Contour plots based on vertical profiles of dissolved (**a**) oxygen (O_2), (**b**) carbon dioxide (CO_2), and (**c**) methane (CH_4) concentrations (μmol L^{-1}) measured at the deepest point of the lake. Inverted triangles in (**a**) show the sampling dates for all profiles and white dots in (**b**, **c**) show the depths sampling resolution for CO_2 and CH_4. Dissolved oxygen concentration was measured at a higher resolution.

3.9 ± 10.4 mmol CO_2 m^{-2} d^{-1} and 44.1 ± 62.0 mmol O_2 m^{-2} d^{-1}). Modeled diffusive CH_4 fluxes were stable during the stratified seasons (May–October), averaging ($\pm$ 1 SD) 0.7 ± 0.4 mmol m^{-2} d^{-1} and 0.7 ± 0.2 mmol m^{-2} d^{-1} for 2016 and 2017, respectively. During fall turnover (November–December), CO_2 and CH_4 fluxes increased drastically, while O_2 fluxes decreased (Fig. 2). This pattern was more pronounced in the second year. Ebullitive CH_4 fluxes were low in winter (both years winter average of 0.1 mmol m^{-2} d^{-1}) and higher in late summer and fall (both summer and fall averages of 0.6 mmol m^{-2} d^{-1}) (Fig. 2b and Supporting Information Fig. S4). Average ($\pm$ 1 SD) CH_4 ebullition between May and October was 0.6 ± 0.3 mmol m^{-2} d^{-1} and 1.0 ± 0.4 mmol m^{-2} d^{-1} for 2016 and 2017, respectively. CH_4 ebullition accounted for 45% and 57% of total summer CH_4 emissions (2016 and 2017, respectively), and about 25% on an annual basis. A summary of annually integrated gas fluxes at the air–water interface for 2016, 2017, and the whole study period are presented in Table 1.

Net gas production rates and annual C balance

Rates of net gas production were highly variable in time (Supporting Information Fig. S5), and covaried among each other (Fig. 3). Whole water column rates of $netO_{2prod}$ were positive during summer months and early autumn when the water column was stratified, and negative during fall and winter months (Fig. 3 and Supporting Information Fig. S5). Rates of $netCO_{2prod}$ (and $netDIC_{prod}$) were almost always positive, except occasionally during the summer, and were negatively

correlated to $netO_{2prod}$ (Fig. 3a). Over the course of the study period, $netCH_{4prod}$ rates were always positive except during late fall and winter where negative $netCH_{4prod}$ shows net CH_4 consumption (Supporting Information Fig. S5). Positive rates of $netO_{2prod}$ and $netCH_{4prod}$ co-occurred during summer stratified periods, while during negative $netO_{2prod}$ the $netCH_{4prod}$ rates were highly variable (Fig. 3b). Annually integrated rates of net gas production are summarized in Table 1.

During the ~ 22 month study period (April 2016–January 2018), Soppensee was a net C emitter to the atmosphere, with CO_2 emissions about 10 times higher than CH_4 emissions (Fig. 4; Table 1). The lake showed positive net ecosystem production on an annual basis (i.e., positive $netO_{2prod}$; biomass and organic matter production). We estimated that about $32\% \pm 26\%$ of the C produced by net ecosystem production (assuming a 1:1 molar conversion from O_2 to C) was converted into net CH_4 production (as methanogenesis minus CH_4 oxidation) which sustained the annual CH_4 emissions (Fig. 4). This $netCH_{4prod} : netO_{2prod}$ ratio varied between years, from $9\% \pm 5\%$ in 2016 to $38\% \pm 30\%$ in 2017.

Discussion

Here, we estimated net gas production rates as a whole ecosystem process that accounts for local production and removal, in addition to potential external inputs and outputs. The different processes in which the various gases are
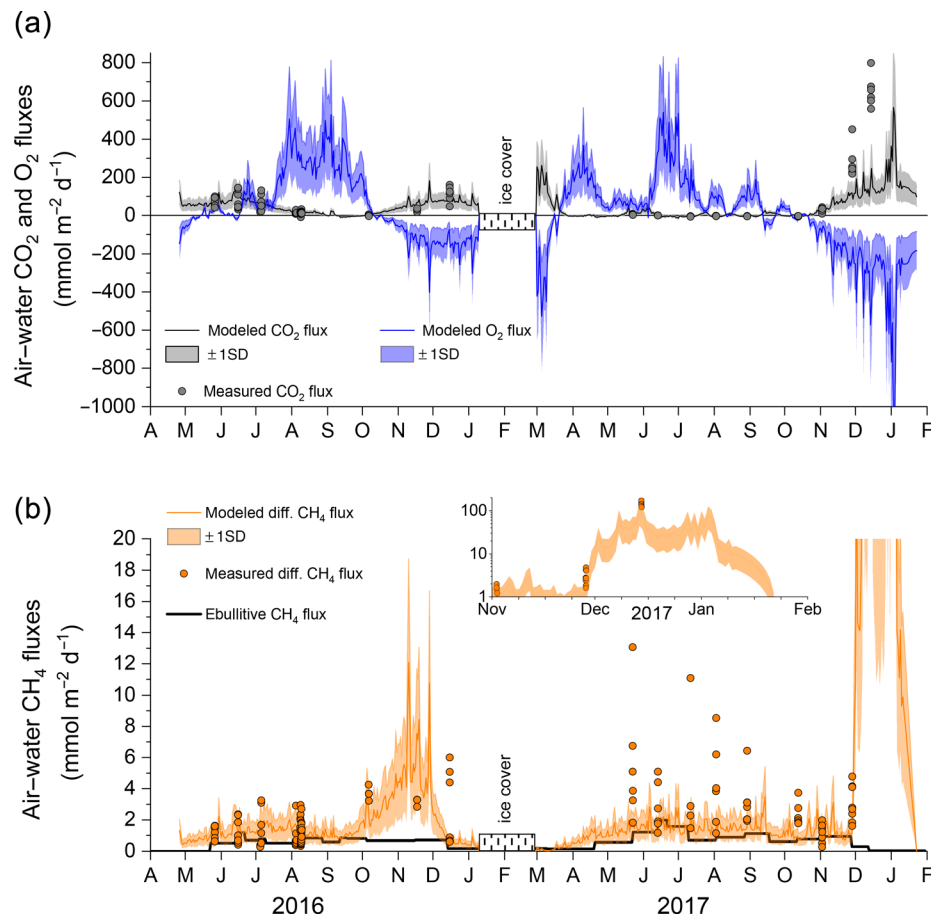
Fig 2. Modeled and measured gas fluxes at the air–water interface during the studied period (2016–2017). (**a**) Diffusive O_2 and CO_2 fluxes with the atmosphere (measured with chambers CO_2 fluxes are the gray circles). (**b**) CH_4 diffusive and ebullitive fluxes (measured diffusive CH_4 fluxes with chambers are the orange circles). Inset in (**b**) shows the November 2017 to January 2018 period on a log scale for better visualization. Lighter colored areas in both panels represent the SD around the mean.

Table 1 Annual air–water gas fluxes and net ecosystem gas production rates ($\pm$ 1SD) in mol m^{-2} yr^{-1} integrated for 2016 (from April 2016 to April 2017), 2017 (from December 2016 to December 2017), and the whole study period (from April 2016 to January 2018). Proportions of ebullition to total CH_4 flux are shown in parentheses.

	2016		2017		Whole period	
	Air–water flux	**Net gas production**	**Air–water flux**	**Net gas production**	**Air–water flux**	**Net gas production**
O_2	14.7$\pm$8.4	15.0$\pm$8.4	5.8$\pm$3.3	4.4$\pm$3.3	5.0$\pm$2.9	4.7$\pm$2.9
CO_2	14.7$\pm$7.9	15.5$\pm$7.9	8.8$\pm$4.9	9.9$\pm$4.9	15.0$\pm$8.1	15.2$\pm$8.1
DIC	—	9.4$\pm$7.7	—	9.9$\pm$4.9	—	14.4$\pm$8.1
CH_4	0.7$\pm$0.3(25%)	1.3$\pm$0.3	1.0$\pm$0.5(24%)	1.7$\pm$0.5	1.6$\pm$0.8(13%)	1.5$\pm$0.8

involved allowed us to explore the various facets of the lake C cycle. We used netO$_{2prod}$ as an estimate of whole-lake net ecosystem production (i.e., net organic matter production) which was comparable to the commonly used O$_2$ diel based method (Supporting Information Section S5). Rates of

netCO$_{2prod}$ (and netDIC$_{prod}$) can be complementary to netO$_{2prod}$, although they also account for anaerobic DIC production and potential C inputs from the catchment. Rates of netCH$_{4prod}$ correspond to the net balance between methanogenesis and CH$_4$ oxidation, while external CH$_4$
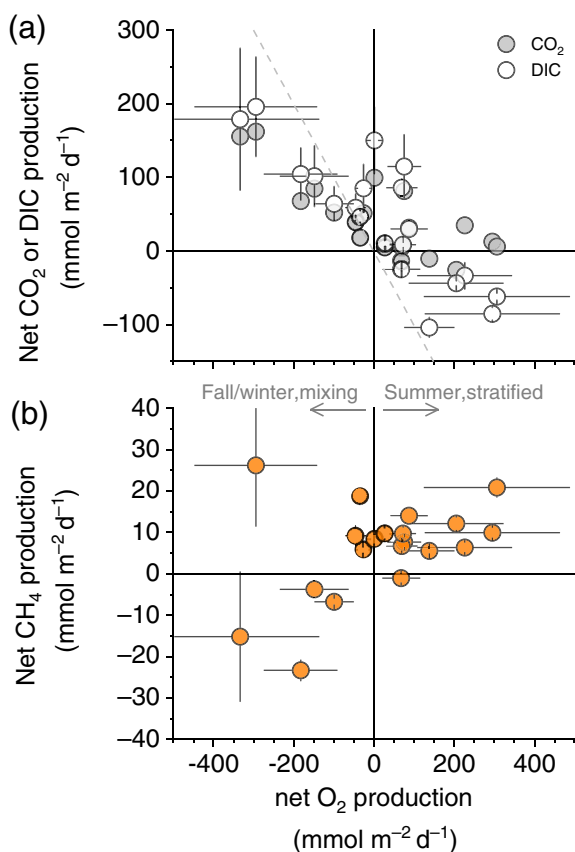
Fig 3. Whole water column net O_2, CO_2, DIC, and CH_4 production rates derived from mass balance calculations for each specific period. (**a**) Net O_2 production relationship with net ecosystem CO_2 (and DIC) production. The dashed gray line is the 1: −1 line. (**b**) Net O_2 production relationship with net CH_4 production. Error bars represent 1 SD.

Fig 4. Summary of the annually integrated net ecosystem O_2 (netO$_{2\text{prod}}$) and CH_4 productions (netCH$_{4\text{prod}}$) and CO_2 and total CH_4 emissions (diffusive and ebullitive) to the atmosphere integrated over the 22 month study period. netCH$_{4\text{prod}}$ is the net balance between gross production and the removal via oxidation in both the sediments and the whole water column. Respiration (R) and production (P) represent cycling between organic carbon (OC) produced using inorganic carbon (IC) occurring in the whole water column and the sediments. To support CO_2 emission and netO$_{2\text{prod}}$, an external C source is needed (dashed arrow). All flux units are in mol m^{-2} yr^{-1}. Over the whole study period, 32% of the organic C produced by netO$_{2\text{prod}}$ was transformed to CH_4 to be emitted via diffusion and ebullition through netCH$_{4\text{prod}}$ (assuming that for 1 mol of O_2 produced, 1 mol of CO_2 is used, and 1 mol of organic C is produced).

inputs did not seem significant (Supporting Information Section S6). Reliable rates of net gas production depend mainly on robust estimates of surface fluxes and gas profile measurements. Achieving these estimates required a few assumptions regarding their spatial and temporal coverage, with implications for net gas production rates (Supporting Information Section S7).

Over the studied period, the lake showed a positive net ecosystem production rate and net CO_2 emissions (Fig. 4, Table 1). Positive net ecosystem production implies net CO_2 removal in the water column; however, there are only a few periods where the lake showed net CO_2 removal in summer (i.e., negative netCO$_{2\text{prod}}$ or netDIC$_{\text{prod}}$; Fig. 3a). If the lake metabolism was entirely driven by aerobic processes and independent from external C inputs, the relationship between netO$_{2\text{prod}}$ and netCO$_{2\text{prod}}$ should be close to the 1 : −1 line (Vachon et al. 2019b). However, both rates did not follow this reference line. At higher netO$_{2\text{prod}}$ rates on the right side of Fig. 3a, the corresponding netCO$_{2\text{prod}}$ rates were relatively higher (above the 1 : −1 line). During these periods, an offset
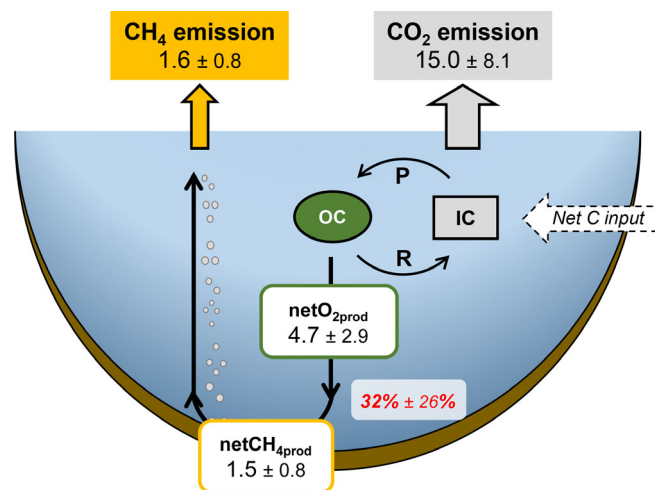
in netCO$_{2\text{prod}}$ compared to netO$_{2\text{prod}}$ can be observed (i.e., y-axis intercept) at about 100 mmol m^{-2} d^{-1} (Fig. 3a). Because of the extent of bottom water anoxia during summer, part of the netCO$_{2\text{prod}}$ offset could have resulted from anaerobic organic matter degradation, which produces CO_2 without consuming O_2 (e.g., denitrification, sulfate reduction, and methanogenesis). This offset could also correspond to external loading of DIC from, for example, groundwater or surface runoff. Either way, external C inputs from surface runoff or groundwater must be provided, in agreement with results from a previous study in Soppensee (Gruber et al. 2000) and several northern lakes (Bogard and del Giorgio 2016). We estimated that 19.7 mol m^{-2} yr^{-1} of additional C would be needed to sustain both CO_2 emissions and netO$_{2\text{prod}}$. Considering the water residence time, this external input would require the C concentration of the inflowing water to be about 5 mmol L^{-1}, which is reasonable since the average DIC concentration in the water column is about 4 mmol L^{-1}.

Lake conditions favorable to CH_4 production are typically characterized by extended anoxia and fresh organic matter supply (Whiting and Chanton 1993; West et al. 2012). In Soppensee, positive rates of netCH$_{4\text{prod}}$ were mainly found during summer and usually co-occurred with periods of

positive $netO_{2prod}$ (Fig. 3b). However, for the resulting fresh organic matter produced in the surface of the lake to be used for methanogenesis certainly requires a time lag. This means that the observed co-occurrence of positive $netO_{2prod}$ and $netCH_{4prod}$ is because both take place during the summer stratified period, where greater light availability favors primary production in the surface and bottom anoxic waters favor methanogenesis. Due to this potential delay, it is thus more likely that some portion of algal-derived organic material produced in summer 2016 (higher $netO_{2prod}$ than in 2017) was then used for methanogenesis in 2017 (higher $netCH_{4prod}$ than in 2016), highlighting the importance of integrating multiple years to account for this legacy effect (Finlay et al. 2019). Taken over the entire study period, the ratio of $netCH_{4prod}$ to $netO_{2prod}$ was about 32%; however, if we use $netO_{2prod}$ from 2016 and $netCH_{4prod}$ from 2017, this ratio becomes 11% $\pm$ 7%. Note that this ratio is not sensitive to the k_{600} used in the calculation since the same k_{600} is used when calculating $netO_{2prod}$ and $netCH_{4prod}$ (Supporting Information Section S8). In terms of GHG, our results suggest that net ecosystem production in Soppensee removed 207 g CO_2 m^{-2} yr^{-1} and $netCH_{4prod}$ produced 396–2080 g CO_2-eq m^{-2} yr^{-1} (using 28–84 as global warming potential of CH_4 over a 100–20 yr time frame). If we assume that methanogenesis mostly uses autochthonous C (West et al. 2012), this loop from $netO_{2prod}$ to $netCH_{4prod}$ (Fig. 4) would represent a GHG release to the atmosphere of about 3–10 times more than the GHG removed by primary production. Due to its greater warming potential, CH_4 dynamics thus become a critical component of this productive lake GHG budget.

There are a few specific conditions occurring in Soppensee that may have favored net CH_4 production, and that may not occur in similar productive lakes. It has been shown in Soppensee that the extended anoxic environment (from 10 m to bottom) promoted methanogenesis and the strong stratification reduced oxidation at the thermocline (Vachon et al. 2019*a*). High O_2 concentrations at the surface and light may in addition inhibit CH_4 oxidation (Shelley et al. 2017; Thottathil et al. 2019). Soppensee also produced CH_4 ebullition at depths deeper than generally expected (> 10 m) (Bastviken et al. 2004; West et al. 2016). However, ebullition at greater depths has also been observed in a meromictic lake (Horn et al. 2017) and is suggested to be caused by the high CH_4 concentration in deeper waters (Langenegger et al. 2019) due to strong thermal stratification (Vachon et al. 2019*a*). Although these specific conditions may suggest that Soppensee is a special case, the C fluxes observed are comparable with other lakes of similar size and trophic status, with CO_2 and CH_4 fluxes within or below the interquartile range of published open water values (DelSontro et al. 2018) (Supporting Information Fig. S6), suggesting that this GHG imbalance could be common among similar lakes.

Conclusions

Enhanced production due to nutrient loading to aquatic systems (i.e., eutrophication) is a major threat for freshwaters ecological functioning and services. Here, we suggest that such productive lakes can emit CH_4 as a result of anaerobic processing of organic matter, which in turn significantly reduces the lake carbon sink. The lake "efficiency" of converting primary production into CH_4 emissions involves several factors that can vary greatly among lakes. Since CH_4 has a warming potential up to 80 times more than CO_2 on a 20 yr period, this lacustrine CO_2 to CH_4 transformation has paramount implications for the global GHG budget. The GHG emission "cost" of eutrophication has hardly been considered until now (Beaulieu et al. 2019) and conclusions from Soppensee suggest the need to investigate more deeply the CH_4 cycling mechanisms in human-impacted freshwater systems.

References

Anderson, N. J., H. Bennion, and A. F. Lotter. 2014. Lake eutrophication and its implications for organic carbon sequestration in Europe. Glob. Chang. Biol. **20**: 2741–2751. doi:10.1111/gcb.12584.

Bastviken, D., J. Cole, M. Pace, and L. Tranvik. 2004. Methane emissions from lakes: Dependence of lake characteristics, two regional assessments, and a global estimate. Global Biogeochem. Cycles **18**: 1–12. doi:10.1029/2004GB002238.

Bastviken, D., L. J. Tranvik, J. A. Downing, P. M. Crill, and A. Enrich-Prast. 2011. Freshwater methane emissions offset the continental carbon sink. Science **331**: 50. doi:10.1126/science.1196808.

Battin, T. J., S. Luyssaert, L. A. Kaplan, A. K. Aufdenkampe, A. Richter, and L. J. Tranvik. 2009. The boundless carbon cycle. Nat. Geosci. **2**: 598–600. doi:10.1038/ngeo618.

Beaulieu, J. J., T. DelSontro, and J. A. Downing. 2019. Eutrophication will increase methane emissions from lakes and impoundments during the 21st century. Nat. Commun. **10**: 1375. doi:10.1038/s41467-019-09100-5.

Bogard, M. J., and P. A. del Giorgio. 2016. The role of metabolism in modulating CO_2 fluxes in boreal lakes. Global Biogeochem. Cycles **30**: 1509–1525. doi:10.1002/2016GB005463.

DelSontro, T., L. Boutet, A. St-Pierre, P. A. del Giorgio, and Y. T. Prairie. 2016. Methane ebullition and diffusion from northern ponds and lakes regulated by the interaction between temperature and system productivity. Limnol. Oceanogr. **61**: S62–S77. doi:10.1002/lno.10335.

DelSontro, T., J. J. Beaulieu, and J. A. Downing. 2018. Greenhouse gas emissions from lakes and impoundments: Upscaling in the face of global change. Limnol. Oceanogr.: Lett. **3**: 64–75. doi:10.1002/lol2.10073.

Finlay, K., R. J. Vogt, G. L. Simpson, and P. R. Leavitt. 2019. Seasonality of pCO_2 in a hard-water lake of the northern

Great Plains: The legacy effects of climate and limnological conditions over 36 years. Limnol. Oceanogr. **64**: S118–S129. doi:10.1002/lno.11113.

Graziani, S., S. E. Beaubien, S. Bigi, and S. Lombardi. 2014. Spatial and temporal pCO_2 marine monitoring near Panarea Island (Italy) using multiple low-cost gaspro sensors. Environ. Sci. Technol. **48**: 12126–12133. doi:10.1021/es500666u.

Gruber, N., B. Wehrli, and A. Wuest. 2000. The role of biogeochemical cycling for the formation and preservation of varved sediments in Soppensee (Switzerland). J. Paleolimnol. **24**: 277–291. doi:10.1023/A:1008195604287.

Günthel, M., D. Donis, G. Kirillin, D. Ionescu, M. Bizic, D. F. McGinnis, H. P. Grossart, and K. W. Tang. 2019. Contribution of oxic methane production to surface methane emission in lakes and its global importance. Nat. Commun. **10**: 1–10. doi:10.1038/s41467-019-13320-0.

Horn, C., P. Metzler, K. Ullrich, M. Koschorreck, and B. Boehrer. 2017. Methane storage and ebullition in monimolimnetic waters of polluted mine pit lake Vollert-Sued, Germany. Sci. Total Environ. **584–585**: 1–10. doi:10.1016/j.scitotenv.2017.01.151.

Jähne, B., K. O. Münnich, R. Bösinger, A. Dutzi, W. Huber, and P. Libner. 1987. On the parameters influencing air-water gas exchange. J. Geophys. Res. Oceans **92**: 1937–1949. doi:10.1029/JC092iC02p01937.

Kelly, C. A., and D. P. Chynoweth. 1981. The contributions of temperature and the input of organic matter in controlling rates of sediment methanogenesis. Limnol. Oceanogr. **26**: 891–897. doi:10.4319/lo.1981.26.5.0891

Langenegger, T., D. Vachon, D. Donis, and D. F. McGinnis. 2019. What the bubble knows: Lake methane dynamics revealed by sediment gas bubble composition. Limnol. Oceanogr. **64**: 1526–1544. doi:10.1002/lno.11133.

Le Quéré, C., and others. 2018. The global carbon budget 2017. Earth Syst. Sci. Data **10**: 405–448. doi:10.5194/essdd-2017-123.

Lotter, A. F. 1989. Evidence of annual layering in Holocene sediments of Soppensee, Switzerland. Aquat. Sci. **51**: 19–30. doi:10.1007/BF00877778.

McGinnis, D. F., J. Greinert, Y. Artemov, S. E. Beaubien, and A. Wüest. 2006. Fate of rising methane bubbles in stratified waters: How much methane reaches the atmosphere? J. Geophys. Res. **111**: C09007. doi:10.1029/2005JC003183.

McGinnis, D. F., G. Kirillin, K. W. Tang, S. Flury, P. Bodmer, C. Engelhardt, P. Casper, and H.-P. Grossart. 2015. Enhancing surface methane fluxes from an oligotrophic lake: Exploring the microbubble hypothesis. Environ. Sci. Technol. **49**: 873–880. doi:10.1021/es503385d.

Myhre, G., and others. 2013. Anthropogenic and natural radiative forcing. *In* T. F. Stocker, and others [eds.], Climate Change 2013: The physical science basis. Contribution of working group I to the fifth assessment report of the Intergovernmental Panel on Climate Change. Cambridge Univ. Press.

Nisbet, E. G., and others. 2019. Very strong atmospheric methane growth in the 4 years 2014–2017: Implications for the Paris Agreement. Global Biogeochem. Cycles **33**: 318–342. doi:10.1029/2018GB006009.

Pacheco, F., F. Roland, and J. A. Downing. 2014. Eutrophication reverses whole-lake carbon budgets. Inland Waters **4**: 41–48. doi:10.5268/IW-4.1.614.

Regnier, P., and others. 2013. Anthropogenic perturbation of the carbon fluxes from land to ocean. Nat. Geosci. **6**: 597–607. doi:10.1038/ngeo1830.

Shelley, F., N. Ings, A. G. Hildrew, M. Trimmer, and J. Grey. 2017. Bringing methanotrophy in rivers out of the shadows. Limnol. Oceanogr. **62**: 2345–2359. doi:10.1002/lno.10569.

Stumm, W., and J. J. Morgan. 1995, *Aquatic chemistry: Chemical equilibria and rates in natural waters*, 3rd Edition. Wiley-Interscience.

Tang, K. W., S. Flury, D. Vachon, C. Ordóñez, and D. F. McGinnis. 2018. The phantom midge menace: Migratory Chaoborus larvae maintain poor ecosystem state in eutrophic inland waters. Water Res. **139**: 30–37. doi:10.1016/j.watres.2018.03.060.

Thottathil, S. D., P. C. J. Reis, and Y. T. Prairie. 2019. Methane oxidation kinetics in northern freshwater lakes. Biogeochemistry **143**: 105–116. doi:10.1007/s10533-019-00552-x.

Tranvik, L. J., and others. 2009. Lakes and reservoirs as regulators of carbon cycling and climate. Limnol. Oceanogr. **54**: 2298–2314. doi:10.4319/lo.2009.54.6_part_2.2298.

Vachon, D., T. Langenegger, D. Donis, and D. F. McGinnis. 2019*a*. Influence of water column stratification and mixing patterns on the fate of methane produced in deep sediments of a small eutrophic lake. Limnol. Oceanogr. **64**: 2114–2128. doi:10.1002/lno.11172.

Vachon, D., and others. 2019*b*. Paired O_2–CO_2 measurements provide emergent insights into aquatic ecosystem function. Limnol. Oceanogr.: Lett. doi:10.1002/lol2.10135.

Vachon, D., T. Langenegger, D. Donis, S. E. Beaubien, and D. F. McGinnis. 2020. Data from: Methane emission offsets carbon dioxide uptake in a small productive lake, v6. Dryad Dataset. doi:10.5061/dryad.3bk3j9kf4

West, W. E., J. J. Coloso, and S. E. Jones. 2012. Effects of algal and terrestrial carbon on methane production rates and methanogen community structure in a temperate lake sediment. Freshw. Biol. **57**: 949–955. doi:10.1111/j.1365-2427.2012.02755.x.

West, W. E., K. P. Creamer, and S. E. Jones. 2016. Productivity and depth regulate lake contributions to atmospheric methane. Limnol. Oceanogr. **61**: S51–S61. doi:10.1002/lno.10247.

Whiting, G. J., and J. P. Chanton. 1993. Primary production control of methane emission from wetlands. Nature **363**: 210–211. doi:10.1038/364794a0.

Yvon-Durocher, G., A. P. Allen, D. Bastviken, R. Conrad, C. Gudasz, A. St-Pierre, N. Thanh-Duc, and P. A. del Giorgio. 2014. Methane fluxes show consistent temperature dependence across microbial to ecosystem scales. Nature **507**: 488–491. doi:10.1038/nature13164.

Conflict of Interest

None declared.